Characterizing stickiness using recurrence time entropy

Matheus Rolim Sales
Michele Mugnaine, José D. Szezech Jr., Ricardo L. Viana, Iberê. L. Caldas, Norbert Marwan, Jürgen Kurths

São Paulo State University (UNESP)

V Workshop on Nonlinear Dynamics

matheusrolim95@gmail.com

May 24, 2024

Summary

Summary

Hamiltonian systems

The time evolution of a Hamiltonian system is given by Hamilton's equations

$$\begin{aligned} \dot{q}_i &= \frac{\partial \mathcal{H}(\mathbf{p}, \mathbf{q}, t)}{\partial p_i} = [q_i, \mathcal{H}], \\ \dot{p}_i &= -\frac{\partial \mathcal{H}(\mathbf{p}, \mathbf{q}, t)}{\partial q_i} = [p_i, \mathcal{H}]. \end{aligned} \tag{1}$$

Any set $(\mathbf{p}, \mathbf{q})$ that satisfies Eq. (1) is said to be canonical and the $2N$ coordinates form a $2N$–dimensional space, called phase space.

Hamiltonian systems have the special property of preserving volume in phase space (Liouville's theorem), *i.e.*, there are no attractors and repellors in the phase space of Hamiltonian systems

Integrable systems

A Hamiltonian system with N degrees of freedom is said to be integrable if there exist N independent constants of motion $f_i(\mathbf{p}, \mathbf{q})$ and if these N constants are in involution, $[f_i, f_j] = 0 \ \forall \ i, j$.

In this case, the dynamics of the system is confined to a N-dimensional *torus*.

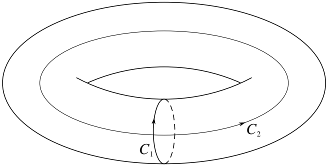

Figure 1: Graphical representation of a two-dimensional *torus*.

Quasi-integrable systems

The phase space of a typical Hamiltonian system is neither integrable nor uniformly hyperbolic.

The Hamiltonian of such a system is given by

$$\mathcal{H}(\mathbf{p}, \mathbf{q}, t) = \mathcal{H}_0(\mathbf{p}, \mathbf{q}) + \epsilon \mathcal{H}_1(\mathbf{p}, \mathbf{q}, t). \tag{2}$$

For small perturbations, the sufficiently irrational *tori* (KAM *tori*) survive the perturbation (KAM theorem), while the rational ones are destroyed.

For two-dimensional systems, the regular and chaotic regions are unconnected domains.

For stronger perturbations, the KAM *tori* are also destroyed and its remnants form a Cantor set, called *cantori*[1].

[1] R. S. MacKay et al., *Phys. Rev. Lett.*, 1984, **52**, 697–700; R. S. Mackay et al., *Physica D: Nonlinear Phenomena*, 1984, **13**, 55–81; C. Efthymiopoulos et al., *Journal of Physics A: Mathematical and General*, 1997, **30**, 8167–8186.

Quasi-integrable systems

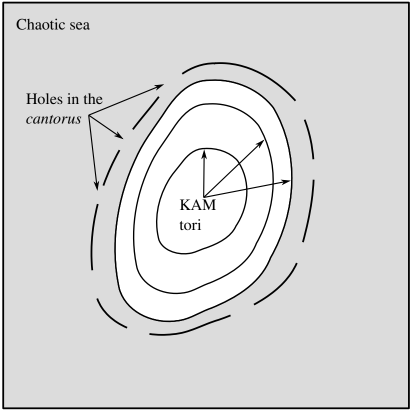

Figure 2: Representation of the phase space of a typical Hamiltonian system, where in gray is the chaotic sea and in white an stability island. Inside the island there are KAM *tori* and around the island are the remnants of a destroyed KAM *torus*, the *cantorus*.

Summary

The standard map[2]

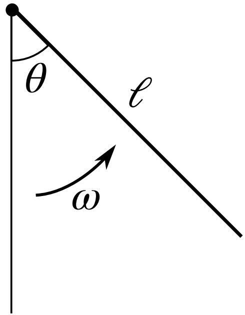

Figure 3: Graphical representation of the kicked rotor.

$$\mathcal{H}(\theta, p, t) = \frac{p^2}{2} - k\cos\theta \sum_n \delta(t-n),$$

$$\theta_{n+1} = \theta_n + p_{n+1} \mod 2\pi,$$

$$p_{n+1} = p_n - k\sin\theta_n.$$

[2] B. V. Chirikov, *Physics Reports*, 1979, **52**, 263–379.

The standard map

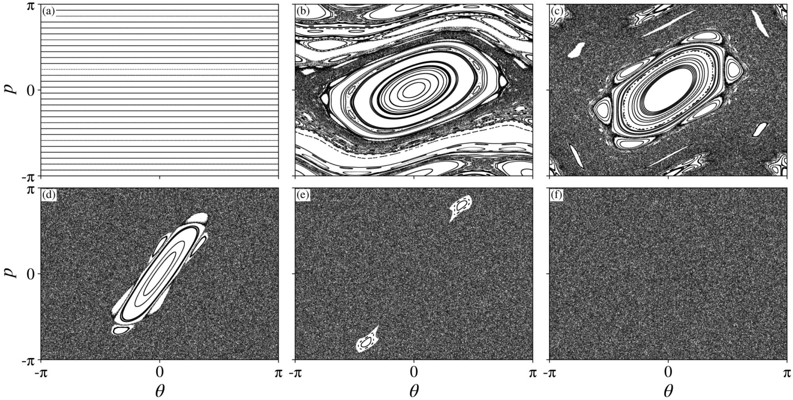

Figure 4: Phase space of the standard map with 100 randomly chosen initial conditions for (a) $k = 0.0$, (b) $k = 0.9$, (c) $k = 1.5$, (d) $k = 3.63$, (e) $k = 5.3$ and (f) $k = 9.0$.

Summary

Recurrence plots

The recurrence plot (RP) was first introduced by Eckmann in 1987[3] and is a graphical representation of the recurrences of time series of dynamical systems.

Given $\mathbf{x}_i \in \mathbb{R}^d$ $(i = 1, 2, \ldots, N)$, the recurrence matrix is defined as

$$R_{ij} = H\Big(\epsilon - \|\mathbf{x}_i - \mathbf{x}_j\|\Big),\ i,j = 1, 2, \ldots, N, \tag{3}$$

where

- N is the time series length;
- $H(\cdot)$ is the Heaviside unit step function;
- ϵ is a small threshold;
- $\|\mathbf{x}_i - \mathbf{x}_j\|$ is the distance in the d-dimensional phase space in terms of a suitable norm.

[3] J. P. Eckmann et al., *Europhysics Letters (EPL)*, 1987, **4**, 973–977.

Recurrence plots

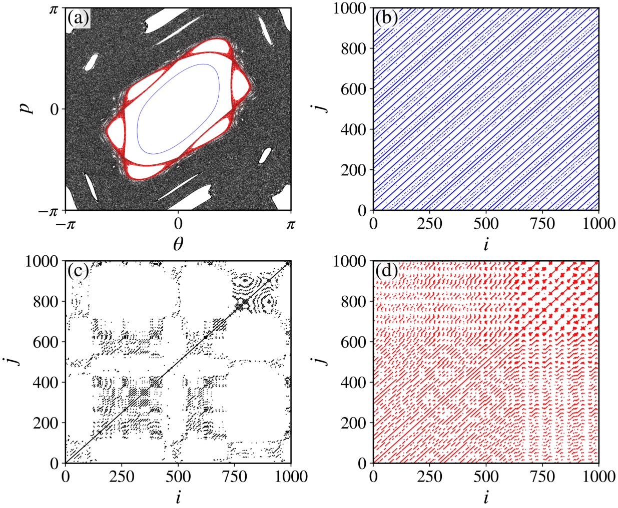

Figure 5: (a) Quasiperiodic (blue), chaotic (black), and sticky (red) orbits, and (b)-(d) their respective recurrence matrix for the first 1000 iterations.

Recurrence quantification analysis (RQA)

Some of the most common RQA measures are[4]:

(i) recurrence rate;

(ii) determinism;

(iii) entropy.

The Shannon entropy of the lines is defined as

$$S = -\sum_{\ell=\ell_{\min}}^{\ell_{\max}} p(\ell) \ln p(\ell), \tag{4}$$

where $p(\ell) = P(\ell)/N_\ell$ is the relative distribution of line segments with length ℓ, and N_ℓ is the total number of line segments.

[4] N. Marwan et al., *Physics Reports*, 2007, **438**, 237–329; N. Marwan, *The European Physical Journal Special Topics*, 2008, **164**, 3–12.

Slater's theorem

The vertical distance between two recurrent points is related to the return times of the orbit[5].

Quasiperiodic orbits can have at most three different return times (Slater's theorem[6]) → $\{\tau_1, \tau_2, \tau_3\}$, where $\tau_3 = \tau_1 + \tau_2$.

It is possible to distinguish between chaotic and regular (periodic and quasiperiodic) dynamics by simply counting the number of unique return times, N_τ, of an orbit[7]:

- $N_\tau = 1$: periodic;
- $N_\tau = 3$: quasiperiodic;
- $N_\tau > 3$: chaotic.

[5] Y. Zou et al., *Chaos: An Interdisciplinary Journal of Nonlinear Science*, 2007, **17**, 043101; Y. Zou et al., *Phys. Rev. E*, 2007, **76**, 016210; Y. Zou, Ph.D. Thesis, Potsdam Univesity, 2007.

[6] N. B. Slater, *Mathematical Proceedings of the Cambridge Philosophical Society*, 1950, **46**, 525–534; N. B. Slater, Mathematical Proceedings of the Cambridge Philosophical Society, 1967, vol. 63, pp. 1115–1123.

[7] M. Mugnaine et al., *Phys. Rev. E*, 2022, **106**, 034203.

Slater's theorem

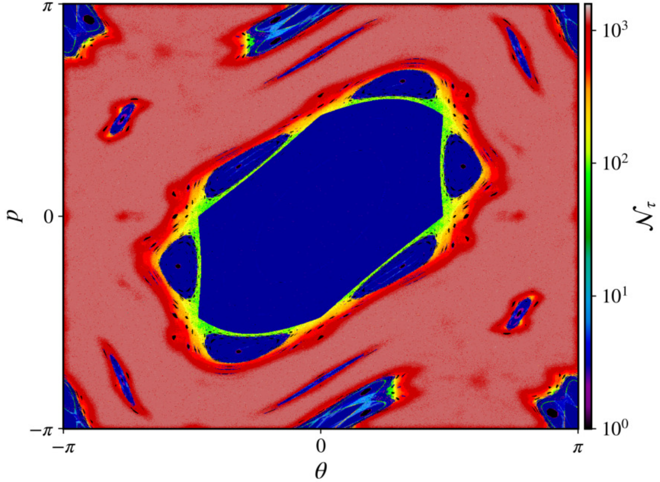

Figure 6: The number of unique recurrence times, $\mathcal{N}_\tau$, for the standard map with $k = 1.5$.

Recurrence time entropy

We use then the relative distribution of white vertical lines, $p_w(v)$, to define the Shannon entropy (4), and the recurrence time entropy (RTE) is defined as

$$\mathrm{RTE} = -\sum_{v=v_{\min}}^{v_{\max}} p_w(v) \ln p_w(v). \tag{5}$$

We can then use the RTE to characterize the dynamics of an orbit:

- periodic orbit (one return time) → RTE = 0;
- quasiperiodic orbit (three return times) → small RTE;
- chaotic orbit (more than three return times) → large RTE.

For sticky orbits we expect a smaller RTE than for chaotic orbits, but larger than it would be for a quasiperiodic orbit.

Recurrence time entropy

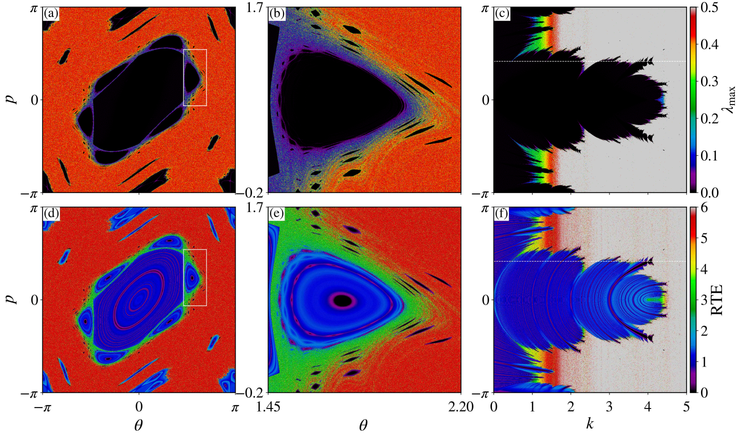

Figure 7: (a)-(c) The λ_{max} and (d)-(f) the RTE for the standard map with $k = 1.5$, for (a), (b), (d) and (e), and with $\theta_0 = 0.0$, for (c) and (f).

Correlation between λ_{max} and RTE

To quantify the correlation between two sets of data, x and y, we use the Person correlation coefficient, defined as

$$\rho_{xy} = \frac{\text{cov}(x, y)}{\sigma_x \sigma_y}.$$

Table 1: Correlation between the λ_{max} and the RTE.

Figure	$\rho_{\lambda_{\text{max}},\text{RTE}}$
7(a) and 7(d)	0.93
7(b) and 7(e)	0.89
7(c) and 7(f)	0.94

Finite-time RTE

Since trapped chaotic orbits behave differently (*e.g.* smaller $\lambda_{\max}$ and RTE), the trappings can be better understood considering the finite-time RTE.

For infinite times, the chaotic orbit fills the entire chaotic component.

We follow the evolution of a single chaotic orbit for a long iteration time and calculate RTE along the evolution of the orbit in windows of size n: $\left\{\mathrm{RTE}^{(i)}(n)\right\}_{i=1,2,\ldots,M}$, $M = N/n$.

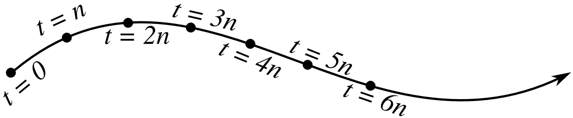

Figure 8: Schematic representation of the evolution of an orbit.

Finite-time RTE

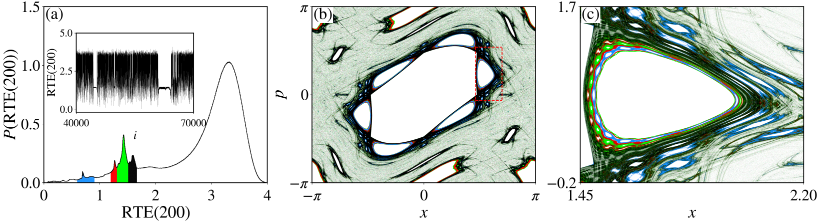

Figure 9: (a) The finite-time RTE distribution for a single chaotic orbit, with $n = 200$, $N = 10^{10}$ and $k = 1.5$, (b) the phase space points that generate the minor peaks in (a) and (c) is a magnification of one of the period-6 satellite islands of (b), indicated by the red dashed lines. The colors in (b) and (c) match the filling colors of (a). Inset: the time series of the FTRTE.

- The inset in Figure 10(a) shows abrupt changes in the value of RTE(200) which cause the distribution to split into more than one mode.
- The multi-modal distribution is due to the hierarchical structure of islands-around-islands.
- When the orbit is in the chaotic sea, RTE(200) is large, corresponding to the largest maximum.
- When the orbit is trapped, the RTE is low and the distribution exhibits smaller maxima for small values of RTE(200).

Cumulative distribution of trapping times

$$Q(\tau) = \sum_{t>\tau} P(t) = \frac{N_\tau}{N_t}.$$

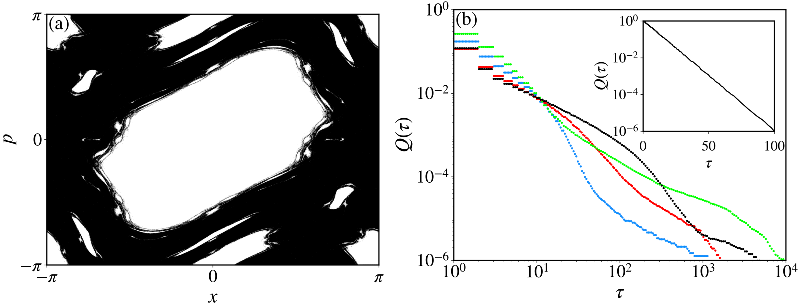

Figure 10: (a) The phase space points that generate the larger peak for high values of RTE in Figure 9(a) and (b) log-log plot of $Q(\tau)$ for each sticky region identified in Figure 9(a) with $N = 10^{11}$ and $n = 200$. Inset: Log-lin plot of $Q(\tau)$ of the phase space points shown in (a). The colors of the dots in (b) correspond to the colors of Figure 9.

Finite-time RTE

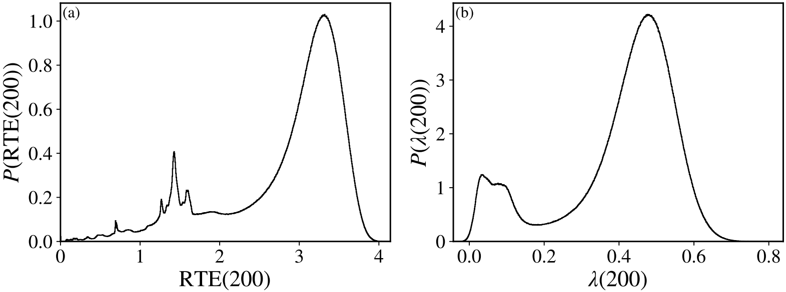

Figure 11: (a) Finite-time RTE and (b) finite-time Lyapunov exponent[8] for $N = 10^{10}$, $n = 200$, and $k = 1.5$.

[8] J. D. Szezech et al., *Physics Letters A*, 2005, **335**, 394–401.

Summary

Drift map

The problem of the $\mathbf{E}\times\mathbf{B}$ drift motion of passive particles can be described through the following two-dimensional, area-preserving mapping[9]

$$\begin{aligned} I_{n+1} &= I_n + \epsilon \sin\left(2\pi\theta_n\right), \\ \theta_{n+1} &= \theta_n + \alpha v_{\parallel}(I_{n+1})\left[\frac{M}{q(I_{n+1})} - L\right] + \gamma \frac{E_r(I_{n+1})}{\sqrt{I_{n+1}}}, \end{aligned} \tag{6}$$

where (I, θ) are the action-angle variables, ϵ is the perturbation strength, and the remaining parameters are taken accordingly to the TCABR tokamak, at the Physics Institute of São Paulo University[10].

The safety factor, $q(I)$, the electric field, $E_r(I)$, and the toroidal velocity, $v_{\parallel}(I)$, are given by the following expressions, compatible with profiles measured on the TCABR tokamak:

$$\begin{aligned} q(I) &= q_1 + q_2 I^2 + q_3 I^3, \\ E_r(I) &= e_1 I + e_2 \sqrt{I} + e_3, \\ v_{\parallel}(I) &= v_1 + v_2 \tanh\left(v_3 I + v_4\right). \end{aligned} \tag{7}$$

[9] W. Horton et al., *Physics of Plasmas*, 1998, **5**, 3910–3917; L. C. Souza et al., *Chaos: An Interdisciplinary Journal of Nonlinear Science*, 2023, **33**, 083132; L. C. Souza et al., *Phys. Rev. E*, 2024, **109**, 015202.

[10] I. C. Nascimento et al., *Nuclear Fusion*, 2005, **45**, 796.

Recurrence plots

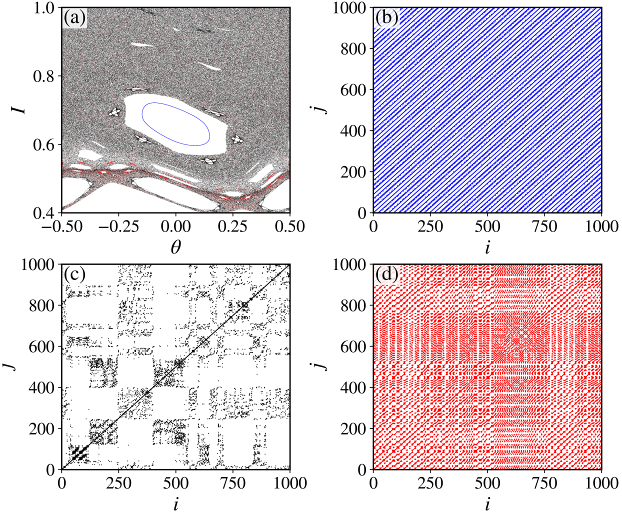

Figure 12: (a) Quasiperiodic (blue), chaotic (black), and sticky (red) orbits, and (b)-(d) their respective recurrence matrix for the first 1000 iterations with $\epsilon = 0.08$.

Finite-time RTE

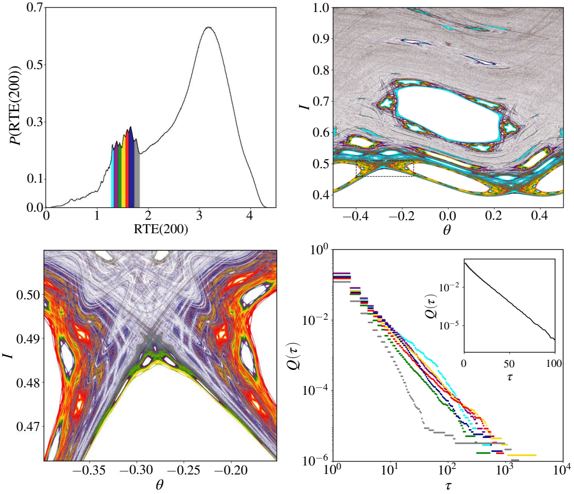

Figure 13: The finite-time RTE distribution for a single chaotic orbit for the drift map, with $n = 200$, $N = 10^{10}$ and $\epsilon = 0.08$, the phase space points that generate the minor peaks, and the cumulative distribution of trapping times for each sticky region.

Summary

Conclusions and perspectives

- The RTE is positively correlated to the largest Lyapunov exponent, with a high correlation coefficient.
- It is possible to distinguish between chaotic and regular solutions using the RTE.
- The peak for small values of $\lambda_{\max}$ in the finite-time Lyapunov exponent distribution is, in fact, composed of several minor peaks, as suggested by Harle and Feudal[11].
- Each peak in the finite-time RTE distribution corresponds to a different hierarchical level in the islands-around-islands structure embedded in the chaotic sea.
- The cumulative distribution of trapping times of each hierarchical level displays a power-law tail, whereas we observe an exponential decay when the orbit lies in the chaotic sea.
- Can the RTE characterize the parameter space of dissipative systems?
- Can the RTE characterize the dynamics of higher dimensional systems?
- Can we define an upper bound for the RTE?

[11] M. Harle and U. Feudel, *Chaos, Solitons & Fractals*, 2007, **31**, 130–137.

Summary

Acknowledgements

CAPES

CNPq

FAPESP
FUNDAÇÃO DE AMPARO À PESQUISA
DO ESTADO DE SÃO PAULO

UEPG
Universidade Estadual
de Ponta Grossa

unesp

PIK

GRUPO DE INVESTIGAÇÃO
Sistemas Complexos e
Dinâmica Não Linear

105 GROUP